GUT3

WP3100: Validation report

Reference:	CLS-DOS-NT-15-038
Nomenclature:	-
Issue:	1. 2
Date:	2015,Apr.29

CLS headquarters
11 rue Hermès
Parc technologique du Canal
31520 Ramonville Saint-Agne
FRANCE

Tel. +33 (0)5 61 39 47 00
Fax +33 (0)5 61 75 10 14
Mail: info@cls.fr
www.cls.fr

CLS Brest Le Ponant
Zone du technopôle de Brest Iroise
Avenue La Pérouse
29280 Plouzané
FRANCE

Tel. 33 (0)2.98.05.76.80
Fax 33 (0)2.98.05.76.90

Chronology Issues:

Issue:	Date:	Reason for change:	Author
1.0	24/02/2015	Creation of the document	Sandrine Mulet (CLS), Frank Siegismund (UH), Per Knudsen (DTU)
1.1	02/03/2015	Modification with correction from Frank and Per	S. Mulet
1.2	29/04/2015	Update with corrections from ESA	S. Mulet

People involved in this issue:

Written by (*):	Sandrine Mulet (CLS) Frank Siegismund (UH) Per Knudsen (DTU)	
Checked by (*):	Stéphanie Guinehut	
Approved by (*):	Gilles Larnicol	
Application authorized by (*):	Stéphanie Limouzin	

**In the opposite box: Last and First name of the person + company if different from CLS*

Index Sheet:

Context:	Validation of GOCE geoid models via ocean's circulation estimation in the frame of the GUT3 project
Keywords:	Geoid Validation MDT ocean current
Hyperlink:	

Distribution:

Company	Means of distribution	Names
ESA	Email	Salvatore Dinardo; Bruno Manuel Lucas; Jérôme Benveniste
DTU	Email	Per Knudsen, Ole Andersen
Hamburg University	Email	Frank Siegismund
Bristol University	Email	Rory Bingham

List of tables and figures

List of figures:

List of Contents

1. OBJECTIVE OF THE DOCUMENT

In the framework of the ESA HPF (High Processing Facility), a number of gravity models have been computed from the GOCE data since the beginning of the mission in 2009. These models use different computational approaches and more and more GOCE data. Since July 2014, the last releases (the 5th) are available and used all the data collected until the end of the mission in November 2013.

The objective of WP3100 is to carry out an independent validation of the GOCE gravity field models for oceanographic application. This document describes the results.

2. INTRODUCTION

Geoid height is a very useful quantity for oceanographers because it gives the contribution in the sea surface height due to gravity. This contribution should be removed from altimetric measurements to end up with the contribution only due to the dynamic of the ocean called dynamic topography. Figure 1a shows the Mean Sea Surface (MSS) CNES-CLS11 [1] that represents a mean of Sea Surface Height from altimetry over 1993 - 1999 time period. The resolution of the MSS is around 10 km. Figure 1b shows geoid height from the release 5 of the GOCE direct method [2] that has a resolution of around 100 km. Both surfaces (geoid height and MSS) have an order of magnitude of some meters while the difference, the Mean Dynamic Topography (Figure 2) have an order of magnitude of some centimetres, 2 order of magnitude smaller. Thus the Mean Dynamic Topography (MDT) is very sensible to errors on geoid model (and MSS), that why looking at MDT is very useful to assess geoid height model. Indeed on Figure 2 one can see omission (due to residual geoid signal in subduction area for instance) and commission errors that should be filtered to have a reliable MDT.

Section 3 studies the impact of MDT assimilation in GECCO numerical model. Section 4 presents assessment of geoid model through computation of MDT and associated mean current and by comparison with unfiltered and filtered drifters (an independent estimate). Section 5 compares GOCE satellite only geoid models with combined geoid model through EOF and spectral analysis. Then section 6 deals with higher resolution.

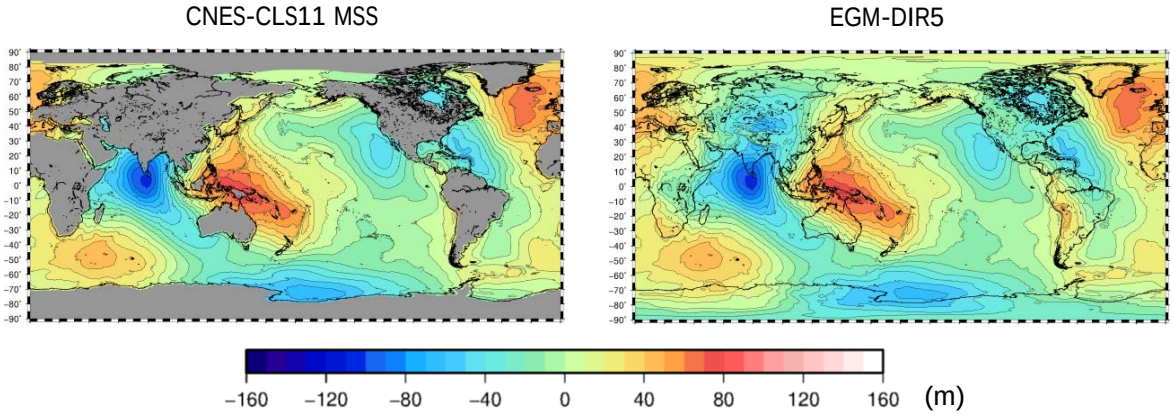

Figure 1: (a) Mean Sea surface CNES-CLS11, (b) Geoid height from the model DIR5

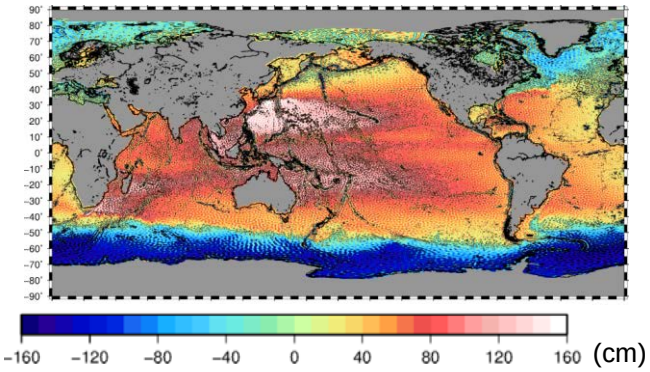

Figure 2: Mean Dynamic topography from the raw difference from MSS CNES-CLS11 and geoid height DIR5

3. VALIDATION OF GOCE MDT THROUGH ASSIMILATION IN NUMERICAL MODEL

In this study we analyse two ocean syntheses, both of which assimilate an extensive data set of ocean observations, but one includes a GOCE MDT as an additional constraint. Results of both integrations are compared in terms of performance of the ocean states estimated. Specifically the modelled MDTs are considered. An upper bound error of the assimilated MDT is provided.

3.1. Computation of geodetic MDT

The MDT used in the assimilation study combines the Mean Sea Surface (MSS) height DTU10 [3] and the first release of the combined GRACE-GOCE geoid solution GOCO01s [4]. Since the period, over which the two optimizations were performed (1993 - 1999), differs from the reference period of the MSS (1993 - 2009), the MSS is re-referenced by subtracting from it the difference in mean sea surface height for those two periods applying AVISO sea surface height anomaly data.

The computation of the MDT follows the Equation 1:

$$MDT = MSS - N$$

Equation 1

with *N* the geoid model. Based on the measurement strategy two sources of errors have to be considered, notably the spectral inconsistency of MSS and geoid model with smaller scales resolved in the MSS (omission error of the geoid), and the commission error of the geoid for short length scales.

The omission error is treated here by spatially smoothing the MSS to the resolution of the geoid (d/o 180) to remove the small scale geoid signal contained in the MSS that would otherwise remain as noise in the MDT after subtracting the geoid. The smoothing is done, following the spectral method described by [5], by transformation to spherical harmonic coefficients, cutting off all coefficients beyond the maximum degree/order of the geoid, and transforming back to physical space.

To diminish the commission error we use a 1.2° spatial Gaussian filter. For consistency reasons the filter is applied not only to the geoid but also to the MSS, and thus simply to the unfiltered MDT that results from Eq. (1).

3.2. GECCO

The GECCO (German contribution to the Estimating the Circulation and Climate of the Ocean) model is based on the Massachusetts Institute of Technology general circulation model (MITgcm; [6]), which is a numerical implementation of the primitive equations formulated on z-levels on a spherical coordinate system. The syntheses use the adjoint method to bring the model into consistency with available hydrographic and satellite data as well as prior estimates of surface fluxes. The set-up we use for the optimizations applies a 1° x 1° grid for the region 80°N - 80°S and 23 vertical levels, and is basically identical to the 50-year run (1952 - 2001) of the GECCO model [7] from which the initial ocean state is taken. Details are provided in [8].

The prior of the atmospheric forcing (downward long-wave radiation, surface air temperature, humidity, precipitation, and the 10 m wind) derives as in the previous estimate from the National Centers for Environmental Prediction (NCEP); these control fields are then adjusted by the method to yield model states that are dynamically consistent with the model physics and the assimilated data within given error limits. As before, the set of assimilated data includes altimeter data, AMSR/E SST, and Argo temperature and salinity profiles. Since the formal geoid error variance is provided as spherical harmonics coefficients, the cost function component for the MDT model data misfit is also evaluated in spherical harmonic space following [9]. To this end the MDT cost function contribution is evaluated in spectral space, and the MDT, consisting of spherical harmonic coefficients of the MDT map, is used as constraint of the modelled topography, which is transformed to spectral space.

3.3. Optimization Setup; Performance of the Ocean State Estimations

Two optimization experiments were performed as part of this study, both covering the period 1993 - 1999. In the first, reference, optimization (henceforth called GECCOref) all data sets were assimilated; however, the MDT was excluded. The second optimization (henceforth called GECCOmdt) is identical to the reference run except that the GOCE-MDT is included as an additional constraint. Both optimizations were continued until the cost function reduction achieved in one iteration step dropped below 0.5 %.

The final reduction of major contributions to the total cost function through the optimization is displayed in Figure 3, showing square root values of relative cost contributions which have been normalized by the number of observations prior to extracting the root. In a solution consistent with the data and the error estimates, the expected values of each of these relative cost contributions would be close to unity. Together the displayed contributions make up 95 % and 93 % of the total cost function for GECCOref and GECCOmdt, respectively. For all shown contributions, the model-data misfits are being reduced more strongly through the optimization that includes MDT. The impact of MDT assimilation is especially strong for the MDT itself (see also Figure 4), but also for the SST (see also Figure 5) and salinity misfits. From the components shown, the one that is least affected is the contribution from Sea Level Anomaly (SLA).

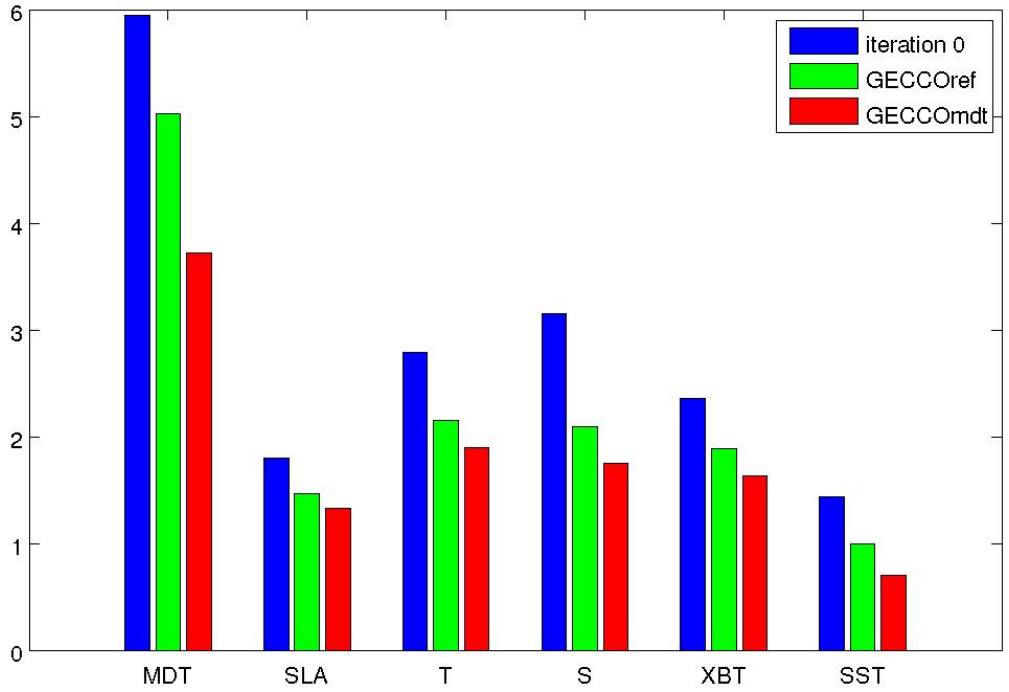

Figure 3: Major contributions to the total cost function diagnosed prior to the optimization (blue), and obtained after the optimizations GECCOref (green) and GECCOmdt (red). Each term was normalized by the respective number of observations prior to taking the square root. In each case the terms shown make up more than 90 % of the total cost function

In comparison to GECCOref, MDT residuals are reduced in GECCOmdt for the Gulf Stream, the Kuroshio Extension, the Equatorial Current Regime and the ACC (Figure 4). In spectral domain, impact of MDT assimilation is especially strong for d/o 11-50 (Figure 6), where residuals of GECCOmdt are considerably lower than for GECCOref.

However, MDT model-data residuals still remain too high in all western boundary currents and the ACC as measured by the relative costs which remain considerably higher than 1 there, i.e., higher than a priori error estimates. We are therefore faced with the conclusion that either the error is too optimistic, or the model is not appropriate (model errors) or the absolute minimum has not been found.

We note that, although the MDT misfits are largely reduced upon its assimilation, the remaining residuals - i.e., the resulting model-data misfits - are considerably larger in some areas than the a priori error estimates and several reasons are possible. The example GECCOref shows that the optimization is unlikely to have converged to the absolute minimum such that further reductions with a modelled MDT is closer to the input MDT are possible. Also, inconsistencies of the input data set for both, the constraints and the control variables might push the solution into a direction away from the realistic MDT. However, there is some evidence that both underestimation of the a priori error and unconsidered model errors contribute to the large residuals.

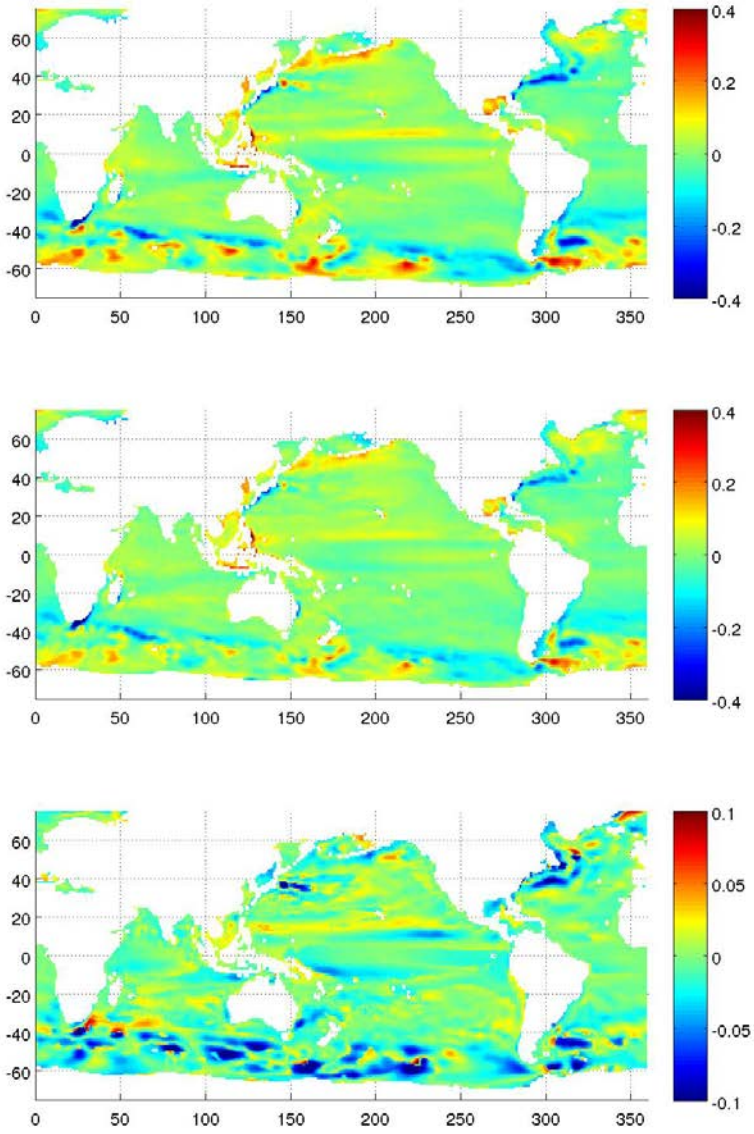

Figure 4: MDT model-data residuals (m) for (top) the GECCOref and (middle) the GECCOmdt experiment (bottom). The difference in absolute model-data residuals (GECCOmdt-GECCOref) is also displayed

The time-mean spatial structures of SST residuals, i.e., the parameter with the second last error reduction are displayed in Figure 7. Model-data biases reduce essentially everywhere upon the assimilation of the MDT constraint, but most noticeable in the South Pacific, South Atlantic, the ACC and the Equatorial Pacific, the Iceland and Greenland Seas, the Gulf Stream and the Kuroshio extension region. On global average, the SST bias reduces from 0.32 to 0.22 K, i.e., by approximately 30 %.

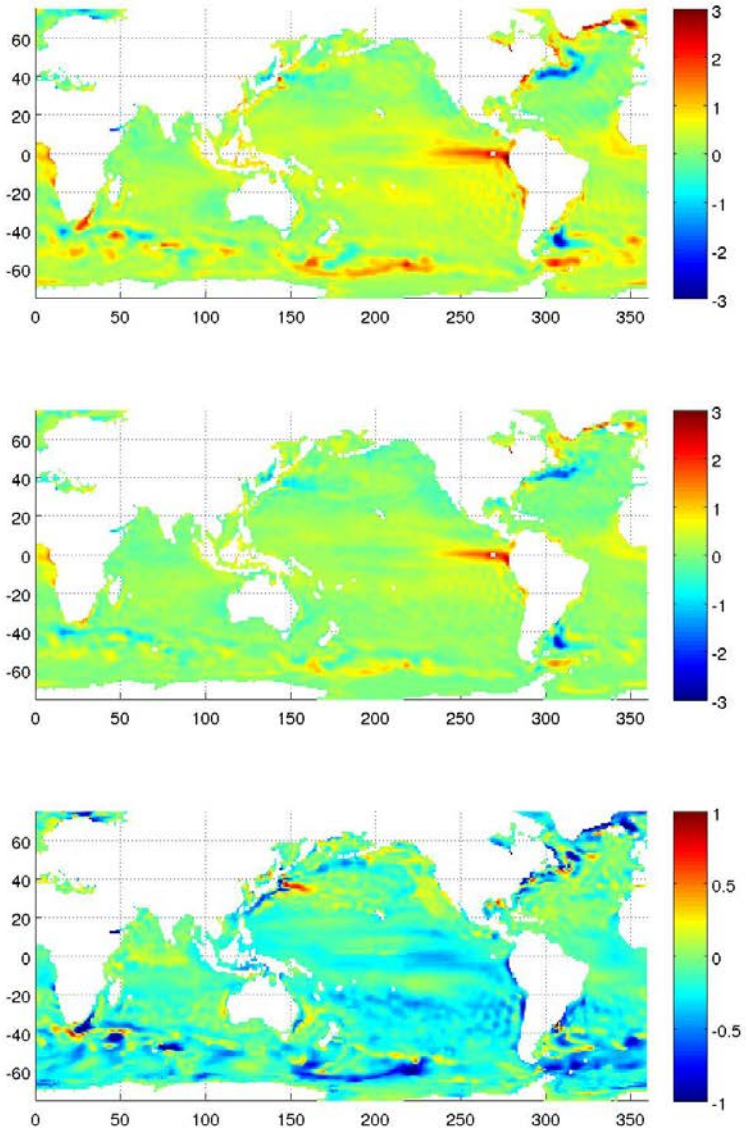

Figure 5: Sea surface temperature model-data residuals (in K) for (top) the GECCOref and (middle) the GECCOmdt experiment (bottom). The difference in absolute model-data residuals (GECCOmdt-GECCOref) is also displayed

3.4. Comparison with drifter velocities

A most direct impact of assimilating the MDT field we expect to emerge from the near surface geostrophic circulation. To test this hypothesis, we evaluated the estimated time-mean surface geostrophic velocities against similar information available from the near-surface drifter velocity observations provided by the Global Drifter Program (GDP; [10]). The comparison of the time mean geostrophic circulation provides insight into both the modelled and the input MDT fields.

Strictly speaking the surface drifter data set is not entirely an independent data set, since a coarse-resolution version of the drifter velocities are being used as constraints. However, the amount of information entering the system is negligible, as the assimilated data set is based on an early

coarse-resolution (2° × 2°) product of the mean surface velocities, which only include a small part of the currently available data [11]. Because associated errors are quite large, a contribution to the total model-data misfit remains below 0.02 %.

To construct an independent time mean geostrophic velocity product from the available drifter data set, the observed drifter velocities were corrected for the non-geostrophic Ekman contribution and (Eulerian) temporal variations. The detailed description of the correction method is provided by [12]. The corrected drifter velocities were originally calculated on a 15' × 15' grid, but for our application they were binned onto the 1° × 1° grid of the OGCM.

To evaluate geostrophic surface currents, we transform model-data residuals into spherical harmonic space. Specifically, geostrophic near-surface currents estimated from 15 m-depth drifter velocities and geostrophic surface velocities derived from the input MDT are compared to the model results. Figure 6 and Figure 7 display the result of the comparison including an intercomparison of the data for the zonal and meridional velocity components, respectively. In all cases, the comparison reveals large differences for long spatial scales up to degree/order 10 (2 000 km and longer), especially for the zonal component. One possible reason for these large differences is strong overestimation of drifter currents due to wind slip after undetected loss of the drogue [13]. However, for scales shorter than 2 000 km (degree/order > 10) the overall difference of the square root of cumulated degree variances between the zonal geostrophic currents obtained from the geodetic MDT and from the drifter data is only 0.7 cm s^{-1}.

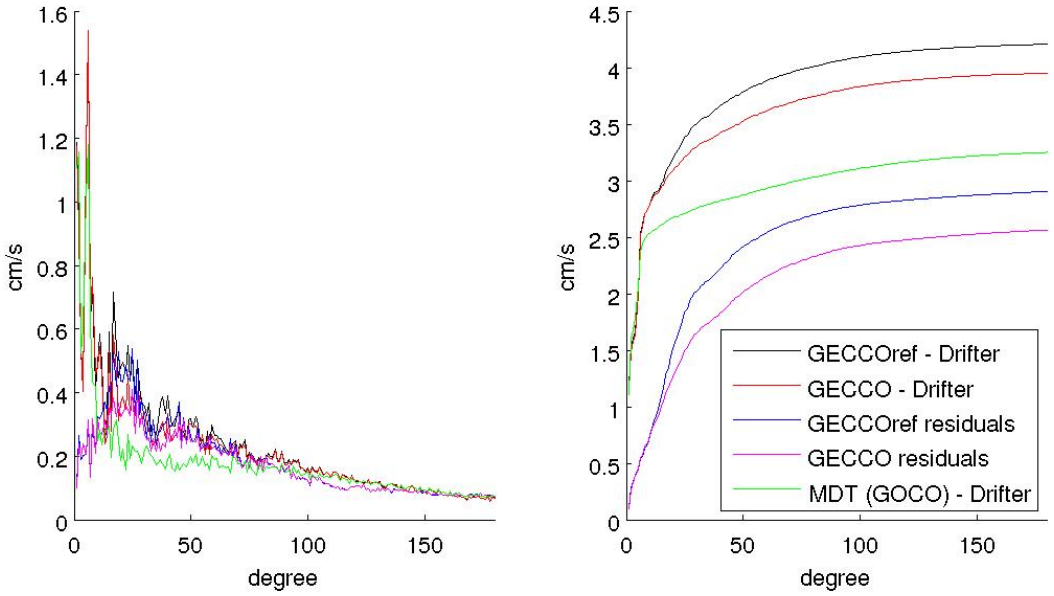

Figure 6: Differences of modeled zonal currents (in cm s-1) to the assimilated MDT (model-data residuals) and to velocities from GDP. In addition, the differences of geostrophic currents from the assimilated MDT to the drifter velocities is displayed. (left) Square root of degree variances, (right) square root of cumulated degree variances

Since the two data sets are essentially independent (despite the use of SLA for re-referencing), their good agreement supports the assumption of a high accuracy for both, the drifter data and the geodetic MDT for scales shorter than 2 000 km. The spectral window, over which the assimilation of MDT impacts on the geostrophic surface circulation, approximately lies between 400 and 2 000 km. For these scales (degree/order 11 - 50) both the residuals and differences of modelled currents to the drifter data are significantly reduced when MDT is assimilated, while for the very long (> 2 000 km) and short scales (< 400 km) the impact of MDT assimilation is weak. This behaviour applies especially for the predominant zonal currents, and less distinct also for the weaker meridional flow.

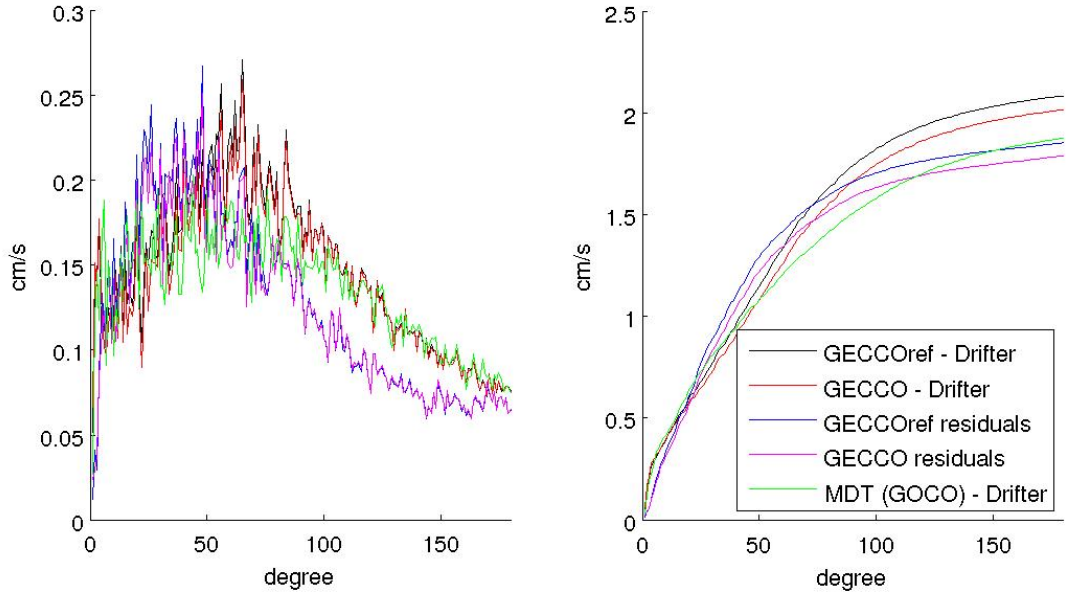

Figure 7: Same as Figure 6, but for the meridional velocity component

The impact of MDT assimilation on the surface geostrophic circulation in physical space is mapped in Figure 8. Currents are drawn closer to drifter observations especially in the equatorial regions of the Pacific and Atlantic, the Western Boundary Currents and the ACC, although peripheral to the areas of reduction often regions with increased residuals exist. Note also that for the small scales, zonal velocities of GECCOmdt are closer to the GOCO MDT than to those from the drifters while for degree/order 11 - 70 GOCO MDT is closest to the drifter velocities.

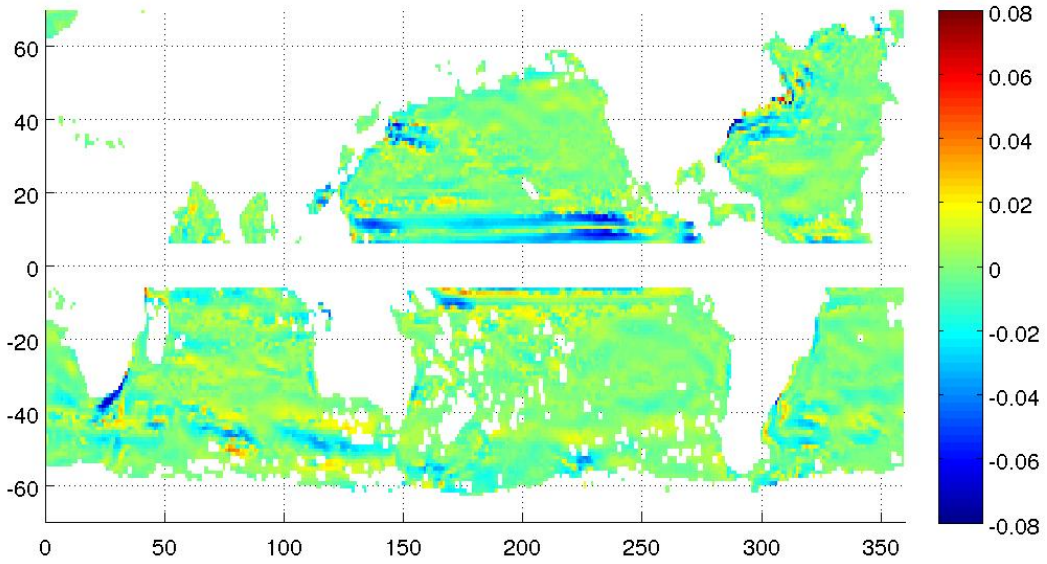

Figure 8: Difference of absolute temporal mean geostrophic surface current residuals (GECCOmdt-GECCOref, in cm s-1). Residuals are calculated as vector differences of modelled geostrophic surface currents and corrected drifter velocities

3.5. MDT error estimate

The optimizations applied in our experiments aim at providing ocean states consistent with the assimilated observational data and the ocean dynamics. The remaining MDT model-data residuals after convergence of the estimated ocean state are used here to estimate the error in the assimilated MDT. In general, the model-data residuals contain errors in the assimilated data sets and model errors. Residuals are overvalued if the synthesis is not fully converged or trapped in a local rather the absolute minimum of the cost function and unrealistic a priori errors might cause the estimated ocean states be biased towards constraints with to low error estimates.

In general, the model-data residuals are expected to over-estimate the true errors due to uncorrelated model errors and since the absolute cost function minimum isn't found in practice. Though we expect the a priori error we provided for the MDT to be probably to low, we don't expect the modelled MDT from the GECCOmdt experiment to be biased toward the assimilated MDT. This assumption is supported by the reduction of residuals in all relevant data sets when the MDT is assimilated, meaning that adjustments in the modelled MDTs towards the assimilated MDT are not bought by increasing costs in other constraints.

As displayed as blue curve in the right panel of Figure 9 the overall MDT model-data residual for the GECCOmdt experiment is 4.5 cm, with the distribution over different length scales provided in the left panel of Figure 9. We consider this as upper bound error for the assimilated GOCE MDT.

However, since due to the resolution of the hydrodynamic model mesoscale activity, its temporal mean signal in the MDT and its nonlinear influence on the large scale mean circulation is not resolved, we expect model errors in regions with high abundance of eddies. If we mask out the ACC south of 60°S and central regions of the Gulf Stream and the Kuroshio, were Eddy Kinetic Energy exceeds 50 $cm^2\ s^{-2}$, and again calculate model-data residuals, we obtain an overall residual of 3.3 cm (Figure 9, red curves) as upper bound GOCE MDT error estimate outside the masked out regions.

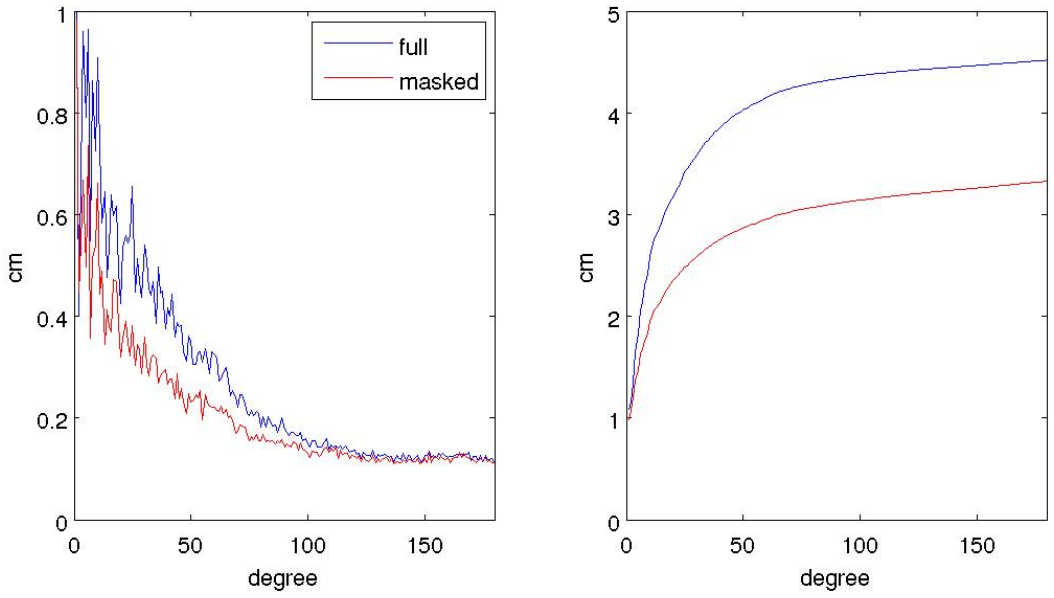

Figure 9: MDT model-data residuals (in cm) for the GECCOmdt experiment. (Left) Square root of degree variances, (right) square root of cumulated degree variances. The blue curves display the original residuals as used in the optimization, while the red curves display the residuals after masking out regions of strong mesoscale activity. See the text for details

It has to be noted, however, that the omission error of the MDT caused by application of the 1.2° Gaussian filter is not considered in our error estimates since the hydrodynamic model, though it has a nominal resolution of 1° (d/o 180), is not sensitive on the smallest scales of its grid due to the numerics applied for the implementation of the hydrodynamic equations.

3.6. Summary

The first release of the combined GRACE-GOCE geoid (GOCO01s) has been applied to compute a geodetic MDT that has been used as constraint in a global ocean synthesis study. The MDT has been assimilated in addition to the extensive ocean in-situ and space-born measurements commonly used in ocean state estimation. The consistency of the MDT with the other constraints has been tested, and comparison to independent observations in terms of near-surface drifter velocities has been performed.

In comparison to a reference synthesis without MDT assimilation but otherwise same configuration, the cost function for all mayor components significantly reduces when the MDT is added as constraint. This applies especially for the MDT and sea surface temperature fields.

The comparison of surface circulation with near-surface drifter data confirms the better representation of the surface circulation when the MDT is included as constraint in ocean state estimation. Considerable improvements are especially found in the zonal currents near the Equator, the ACC and the Western Boundary Currents.

4. COMPARISON WITH DRIFTERS

4.1. Method

In order to investigate the quality of the new GOCE geoid models we use the same method that the one described by [14], [15] and [2]. We have computed MDTs from releases 2 to 5 from the direct method (DIR) and the last release of the time-wise method (TIM5). To quantify the improvement of GOCE relative to GRACE mission we have also computed MDT from ITG-Grace2010s [16]. The MDTs are computed by subtracting the different geoid models from MSS CNES-CLS11. As mentioned in the introduction, the raw MDTs have to be filtered. We applied a Gaussian filter using for the resolution scales five different values (80, 100, 125, 150 and 200 km). Then we compute associated mean geostrophic currents deduced from the MDT gradients called geodetic currents in the following.

These currents are compared with independent estimates (called drifter currents in the following) that are deduced from all the 15-meter drogued drifting buoy data collected from 1993 to 2012 in the framework of the international Surface Velocity Program. These data are distributed by AOML where they first have been quality controlled and krigged [17] in order to provide 6-hourly velocity measurements. In order to extract from the drifting buoy velocities only the geostrophic component, the Ekman current was first modelled ([18], [19]) and substracted. Then, a 3 day low pass filter was applied to the velocities to remove inertial and tidal currents as well as residual high frequency ageostrophic currents. Finally the geostrophic velocity anomalies deduced from the Sea Level Anomalies from AVISO [20] relative to the 1993 - 1999 period are interpolated along the drifter's trajectories and substracted from the associated instantaneous geostrophic currents to have an estimate of the mean geostrophic currents relative to the same 7-year period. The observations are then averaged in ¼° boxes.

The drifter currents obtained as described above are used without any filtering (section 2.2) or filtered at the same resolution scales and using the same Gaussian filter than the MDTs computed

from geoid models. Standard deviations of the differences between the geodetic currents and drifter currents are computed at different resolution scales.

4.2. Unfiltered drifters (assessment of omission and commission errors)

Comparison to unfiltered drifter currents gives estimate about commission error but also omission error. That why when the resolution decreases the standard deviations first decrease a lot (for instance from 80 to 100 km, see Figure 10) at the same time that noise is removed. Then the standard deviations increase again because useful oceanic signal is removed from geodetic current while it is seen by the drifters. The optimal resolution for which we filter enough noise but keep as much oceanic signal as possible is the one that minimises the standard deviation of the difference. The optimal resolution is 150 km for ITG-Grace2010 while is 125 km for the first GOCE releases and is going closer and closer to 100 km with the last releases (Figure 10). Note also how the standard deviations decrease at 100 km from GRACE to DIR2, then from DIR3 to DIR4 thanks to the reprocessing of the GOCE data and then from DIR4 to DIR5 thanks to the lowering of the GOCE orbit.

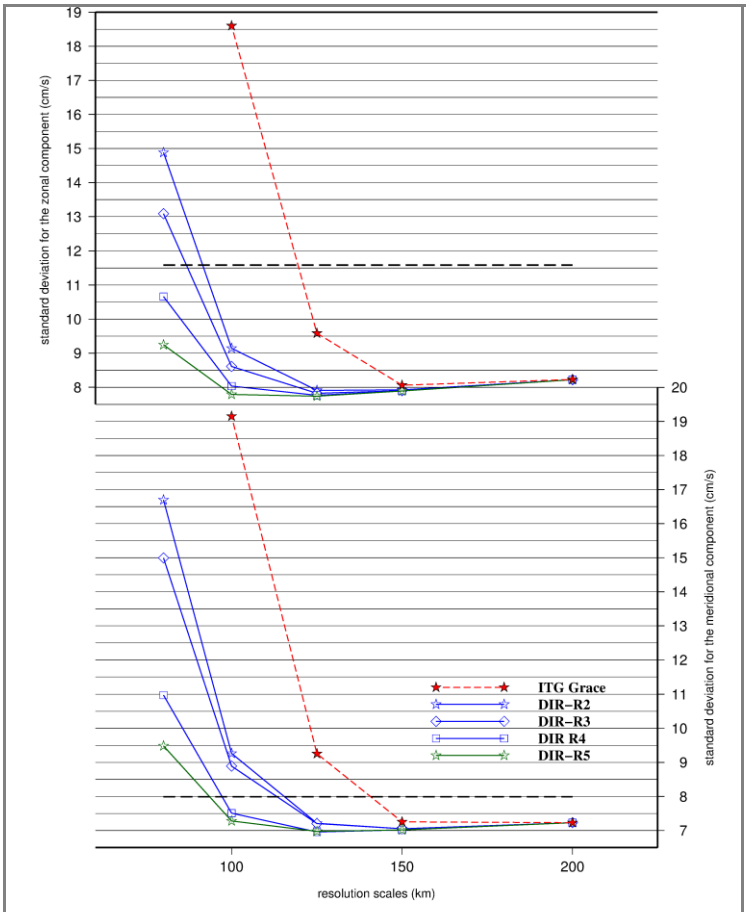

Figure 10: Global standard deviation of the difference between geodetic current and unfiltered drifter estimate for (top) zonal and (bottom) meridional component (cm/s). The black dotted lines show the standard deviation of the unfiltered drifter estimate.

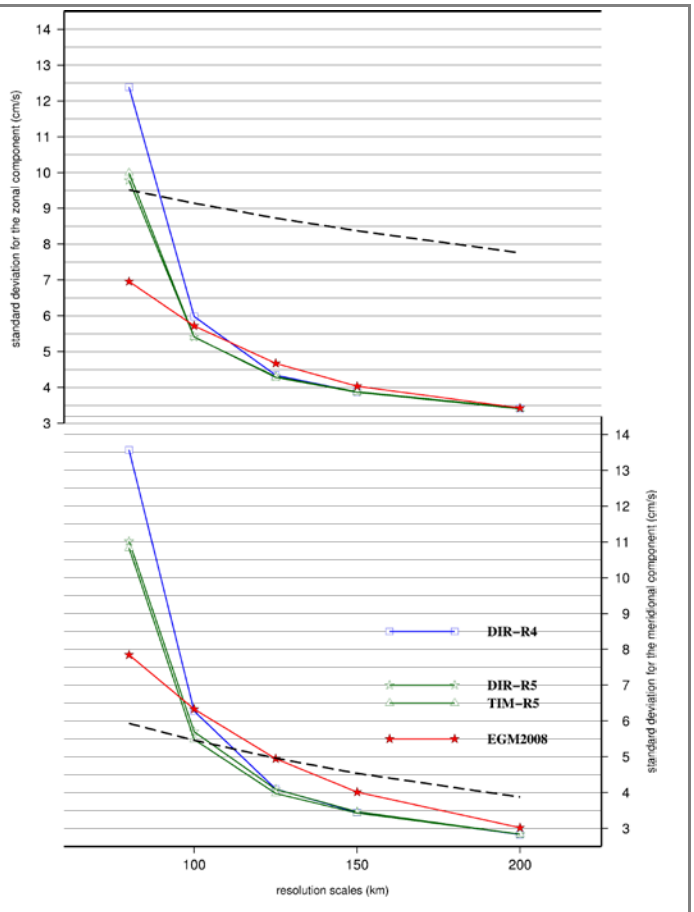

Figure 11: Global standard deviation of the difference between geodetic current and filtered drifter estimate for zonal (top) and meridional (bottom) component (cm/s). The black dotted lines show the standard deviation of the filtered drifter estimate.

4.3. Filtered drifters (assessment of commission errors only)

Comparison to filtered drifter currents takes only into account the commission error. Figure 11 shows that both methods, direct and time-wise, have similar performances. At 100 km the standard deviation of the difference is 5 cm/s. This is an overestimation of the error due to geoid error and includes around 3 cm/s on drifter velocity estimate and some centimetres on MSS. Note also that velocities (gradients of the height) are much more sensible that height itself and that we use Gaussian filter that is not an ideal filter.

Figure 12 and Figure 13 show the regional comparisons with drifters at 125 km of resolution. The RMS of the difference for zonal component is everywhere less than 100 % of the signal and is even almost everywhere less than 20 %. However, the meridional component is much more challenging because the oceanic signal is smaller. Indeed, in most of the Pacific the RMS of the difference is more than 100 %. But in North Atlantic and in the circumpolar current the RMS is less than 40 %.

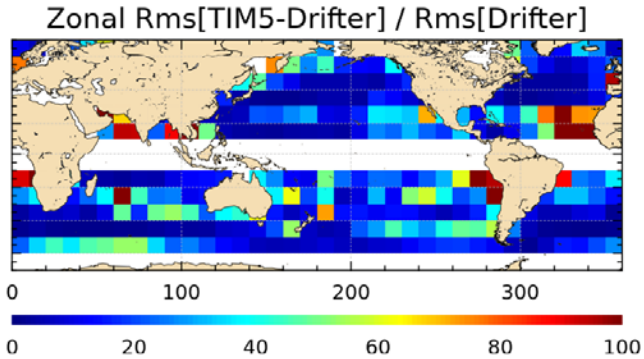

Figure 12: RMS of the difference between geodetic zonal current from TIM5 and drifters estimate both filtered at 125 km. This quantity is computed in 10° by 10° boxes and is express as percentage of the RMS of the drifters (%)

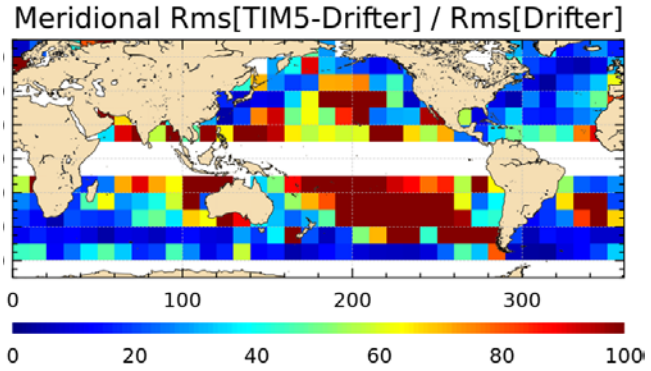

Figure 13: Root Mean Square (RMS) of the difference between geodetic meridional current from TIM5 and drifters estimate both filtered at 125 km. This quantity is computed in 10° by 10° boxes and is express as percentage of the RMS of the drifters (%)

On Figure 11 we also consider combined geoid model EGM2008 that does not include GOCE data but resolves small scales thanks to terrestrial gravity data as well as marine gravity information obtained from altimetry data. The results show that the tested geoid models that include GOCE data give better results than EGM2008 between 100 and 200 km. Thus data obtained from GOCE definitely improve the MDT. However at 80 km and smaller scales, MDTs computed from satellite only geoid models do not perform well since these scales are not resolved.

5. COMPARISON OF GOCE GEOID MODELS WITH MEAN SEA SURFACE, SPECTRAL ANALYSIS

In this study, a series of GOCE geoid models are compared with the DTU13MSS mean sea surface to assess the quality of the GOCE models. In oceanographically quiet areas with very little ocean dynamics, the mean sea surface and the geoid may be assumed to be similar, except for a very smooth topography signal. Then the residuals are analyzed by computing Fourier power spectra to identify and characterize the dominant features.

5.1. Method

The analysis was carried out using differences between the mean sea surface DTU13MSS and a number of GOCE geoid models This was done in a quiet 30 x 30 deg. area in the South-eastern Pacific using the following gravity models:

- tim_r3,
- tim_r4,
- tim_r5,
- dir_r3,
- dir_r4,
- dir_r5,
- eigen-6c,
- eigen-6c2,
- eigen-6c3.

It should be noted that the TIM and the DIR models are satellite only models and that the EIGEN models are combination model that include terrestrial gravity information and are expanded to a much higher degree and order. Also, it should be noted that the terrestrial gravity at sea for the EIGEN models are obtained from satellite altimetry.

In this part of the assessment an EOF decomposition [21] of the differences was carried out to extract and characterize the dominant features and associate them with different gravity models. The EOF analysis done using a singular value decomposition that expands the differences into orthogonal functions – one set of orthogonal spatial functions describing the common features and one set of orthogonal weights associated with each of the gravity models.

A study of the Fourier power spectra shows the main differences between the GOCE models in their fit to the mean sea surface are associated with wavelengths between harmonic degrees 100 and 200. Subsequently, a larger number of GOCE models were compared with the DTU13MSS to derive a measure for quantifying the quality of the various GOCE models. That analysis was carried out using the following 23 models:

- spw_r2,
- tim_r2,
- dir_r2,
- goco02s,
- dgm1s,
- eigen6s,
- eigen6c,
- tim_r3,
- dir_r3,
- goco03s,
- eigen6c2,
- dir_r4,
- tim_r4,
- itg-goce02,
- gogra02s,
- jyy_goce02s,
- eigen6c3,
- eigen6s2,
- gogra04s,
- jyy_goce04s,
- dir_r5,
- tim_r5,
- eigen6c4.

Furthermore this analysis was carried out in three additional quiet areas. Those are 30 by 30 degree areas in the Northeast Pacific, the Northeast Atlantic and the Southeast Atlantic oceans.

5.2. Results

The first EOF tends to absorb the mean field of the surfaces entering the analysis. In this analysis the first EOF spatial function is shown in Figure 14.

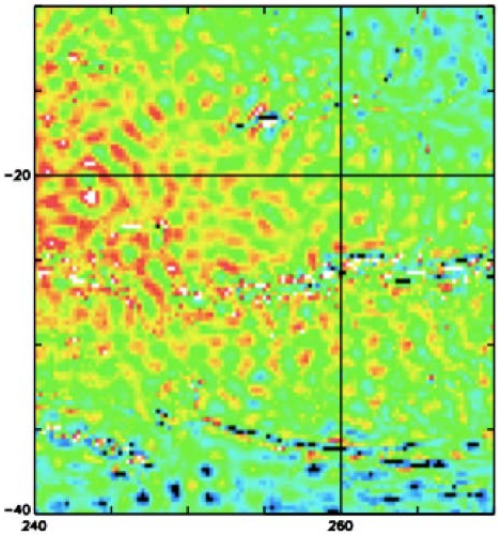

Figure 14: The first EOF spatial function

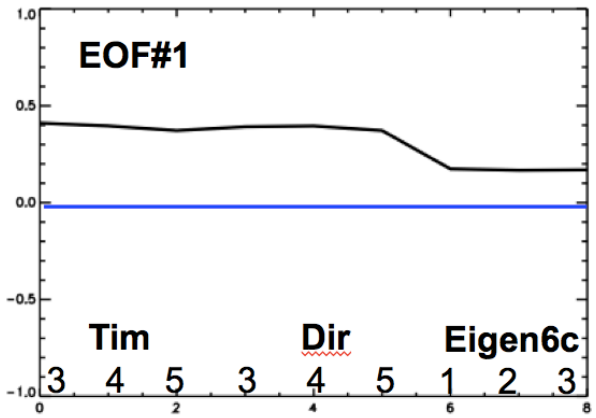

Figure 15: The weights associated with the first EOF

The first EOF function shows the general feature of the differences between the MMS and the tested geoid models. As displayed in Figure 14 those are mainly characterised by short wavelength features associated with the omission geoid errors, i.e. parts of the geoid that are not resolved by the gravity models. In additions a small smooth signal associated with the mean dynamic topography is seen.

In Figure 15 the associated weights (or loadings) are shown. From those it is evident that the features are common features in all satellite only GOCE models, i.e. the TIM and the DIR models. The EIGEN models have less content associated with EOF 1.

The second EOF spatial function is shown in Figure 16. It basically shows short wavelength features only. The 2D power spectrum of the spatial function is shown in Figure 17. It displays the characteristic isotropic ring of high values. The high values are associated with wavelengths between 0.4 and 0.8 cycles per degree roughly corresponding to harmonic degrees 150 - 250.

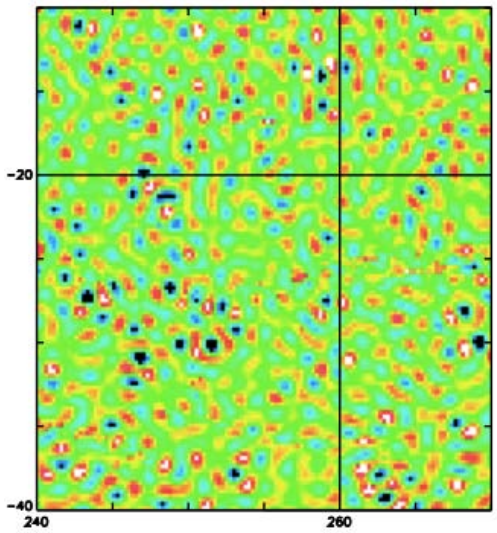

Figure 16: The second EOF spatial function

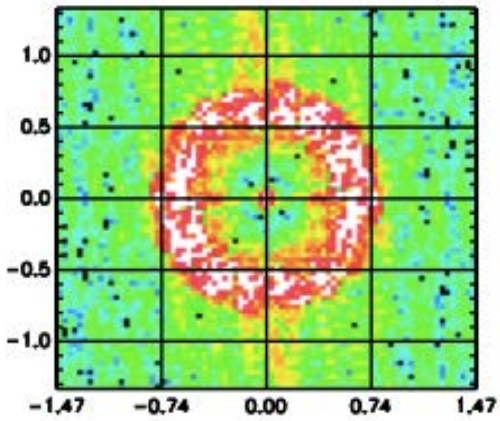

Figure 17: 2D power spectrum of the spatial function associated with the second EOF

The weights of EOF#2 are shown in Figure 18. They show that this EOF is associated with the different releases of the satellite only models and show the progression from release 3 to release 5 in a similar way for both the TIM and the DIR models. Hence, this EOF describes the improvements of the TIM and the DIR models as more GOCE data became available. There is very little influence on the EIGEN models.

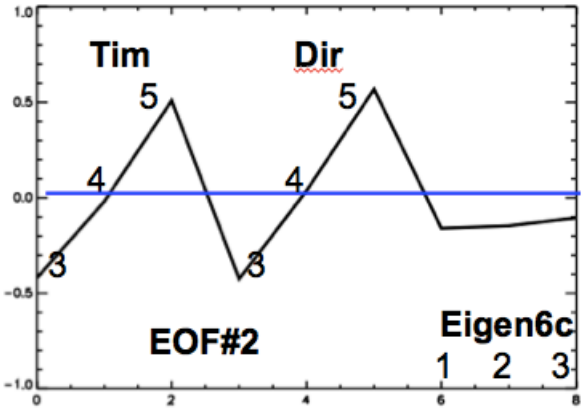

Figure 18: The weights associated with the second EOF

The third EOF spatial function is shown in Figure 19. It basically shows a similar pattern as the first EOF. The details associated with the short wavelength features have the same sign as in the first EOF. The smooth large-scale feature, however, is reversed.

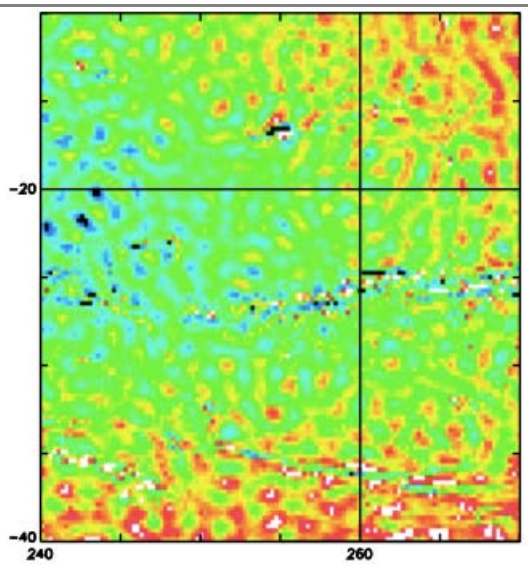

Figure 19: The third EOF spatial function

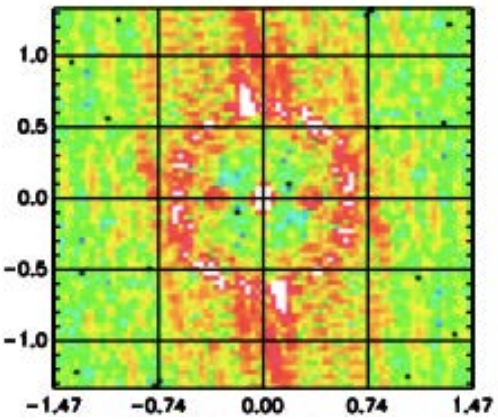

Figure 20: 2D power spectrum of the EOF#3 spatial function

The 2D power spectrum (Figure 20) shows the characteristic isotropic ring of high values associated with wavelengths of between 0.5 and 0.8 cycles per degree roughly corresponding to harmonic degrees 180 - 250. Outside the ring, two tales are seen. They are associated with the very short scale features of the east-west going structures. Inside the ring, two spots of high values are seen. They are associated with wavelengths around 0.3 cycles per degree in the east-west direction and around zero in the north-south direction. This corresponds to harmonic degrees and orders around 110.

The weights of EOF#3 (Figure 21) show little influence on the satellite models. EOF#3 is clearly associated with the EIGEN models. The negative weights indicate this EOF relative to EOF#1 enhances the long wavelength signal and reduces the short wavelength features seen in the spatial function of EOF#1. Hence, EOF#3 describes the enhanced MDT and the reduced omission errors in the EIGEN model. However, EOF#3 also show that the EIGEN models have some north-south going stripes associated with harmonic degrees and orders around 110 included. They may probably be associated with problems in the GRACE data.

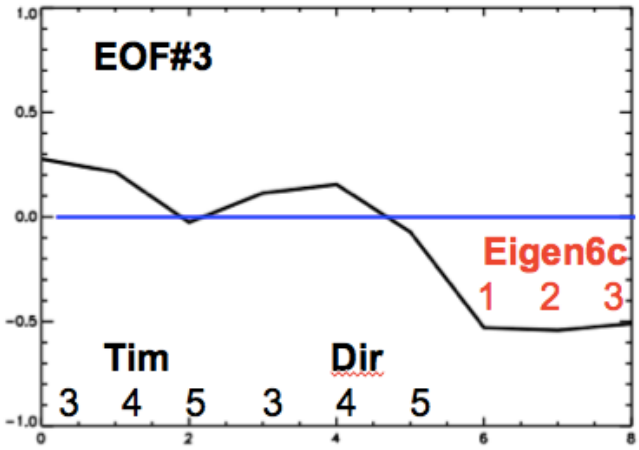

Figure 21: The weights associated with the third EOF

Subsequent to the EOF analysis a direct comparison of the TIM rel.5 and the EIGEN-6C3 was carried out. The two differences are shown in Figure 22. The differences between the models (satellite only

and combination) which also the EOF analyses identified and described in EOF#3, are clearly seen. For the TIM model the omission errors are quite visible; for the EIGEN model the differences display a smooth surface.

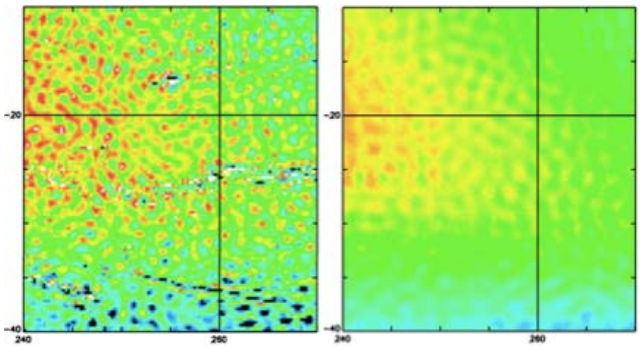

Figure 22: Differences MSS and TIM (left) and EIGEN (right) (same colour scale)

The 2D power spectra (shown in Figure 23) show similar isotropic rings of high values. However, for the EIGEN model, the values are lower. Especially outside the ring (at 0.55 cycles per degree ~ harmonic degree 200) the EIGEN model give much lower values without the an-isotropic tails.

The rotationally averaged isotropic spectra are shown in Figure 24. They show distinctly this reduction.

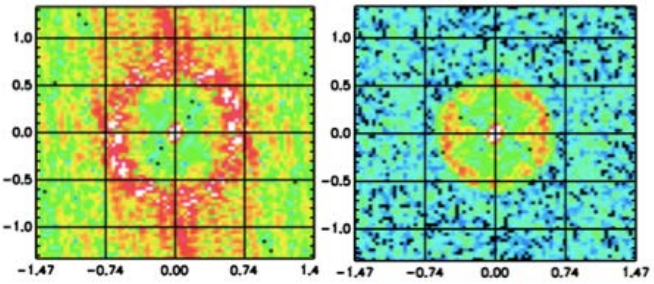

Figure 23: 2D power spectra of differences MSS and TIM (left) and EIGEN (right) (same colour scale)

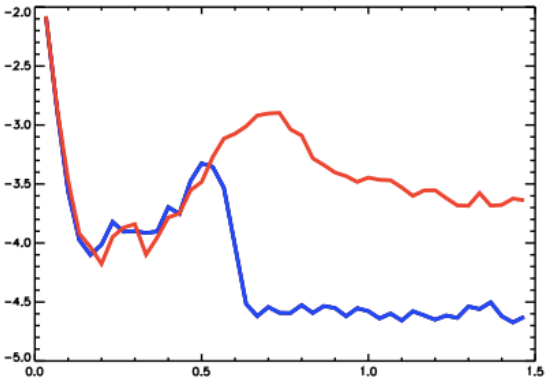

Figure 24: Rotationally averaged isotropic spectra associated with TIM r5 (red) and EIGEN-6C3 (blue)

In addition, rotationally averaged isotropic power spectra of the differences obtained using the satellite only models were derived to investigate the effects of adding more data to the various models for both the TIM and the DIR models. The spectra clearly display (Figure 25) the evolution of the models from releases 3 through 5. Mainly at wavelengths associated with 0.4 - 0.7 cycles per degree (roughly corresponding to harmonic degrees 150 - 250) the fit to the mean sea surface improves significantly.

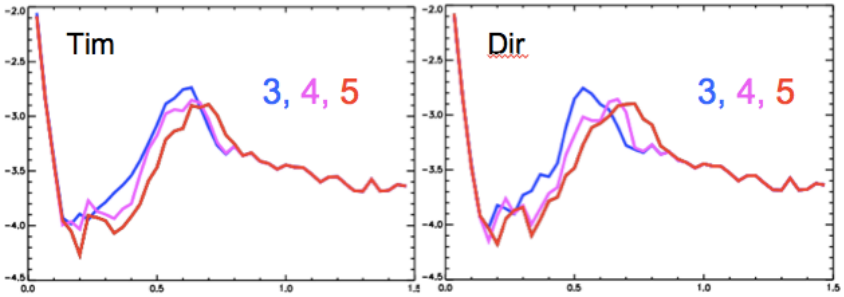

Figure 25: Isotropic power spectra of differences obtained using the TIM models (left) and the DIR models (right) for releases 3 (blue), 4, and 5 (red)

The study of the Fourier power spectra shows the main differences between the GOCE models in their fit to the mean sea surface are associated with wavelengths between harmonic degrees 100 and 200. Subsequently, a larger number of GOCE models were compared with the DTU13MSS to derive a measure for quantifying the quality of the various GOCE models. That analysis was carried out using the 23 models mentioned above in four quiet 30 by 30 degree areas: The Southeast Pacific (SEP), the Northeast Pacific (NEP), the Northeast Atlantic (NA) and the Southeast Atlantic oceans (SA).

The results are shown in Figure 26. The results clearly show the progressive improvements in the models as more data become available. The results also show the improved fit of the EIGEN models.

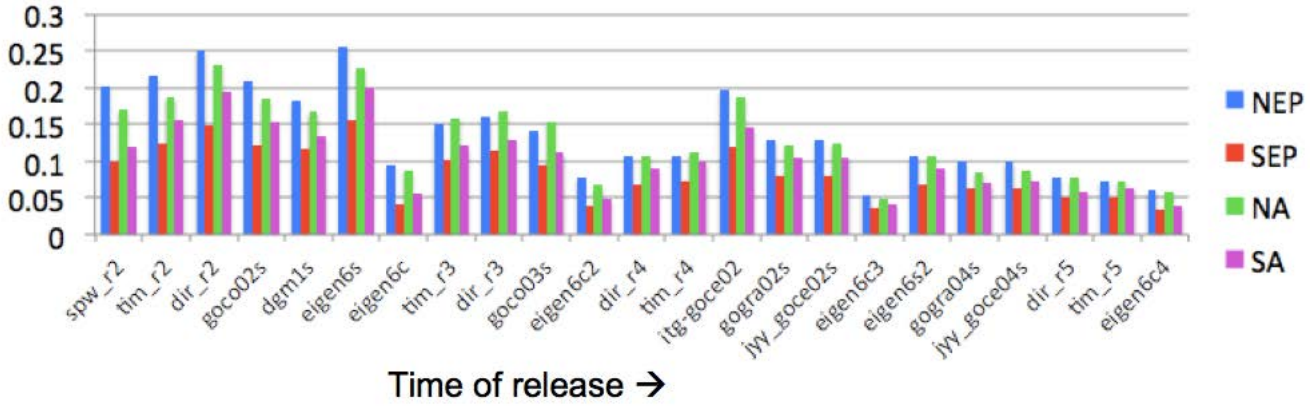

Figure 26: Accumulated differences between GOCE geoid models and DTU13MSS from harmonic degree 100 to 200 over 4 areas: Southeast Pacific (SEP), the Northeast Pacific (NEP), the Northeast Atlantic (NA) and the Southeast Atlantic oceans (SA)

Then the results in the four areas were averaged for each model, sorted and displayed as well. This result is shown in Figure 27. As expected, the release 5 modes together with the combinations are producing the lowest values.

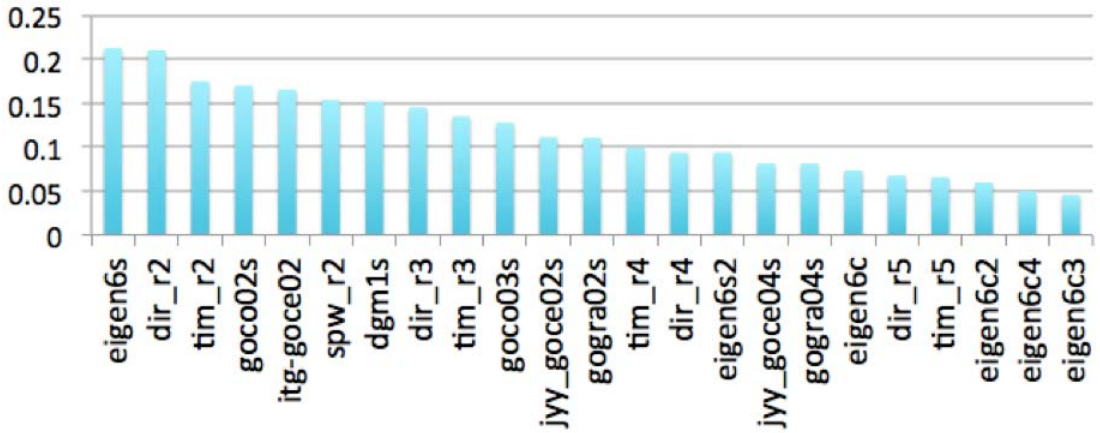

Figure 27: Average over the 4 areas of the accumulated differences between GOCE geoid models and DTU13MSS from harmonic degree 100 to 200

5.3. Summary

Nine GOCE models have been assessed using a mean sea surface derived from satellite altimetry in a quiet ocean area in the Southeast Pacific. The results obtained using both EOF and Fourier spectral analysis show clearly and efficiently the features that are relevant to consider in such comparisons. The differences between the satellite only models and the combination models are evident at wavelengths shorter than what corresponds to harmonic degree 200. Here the integration of altimetric gravity anomalies in the combination models makes the geoid models fit the mean sea surface at those wavelengths. For the satellite only models the differences are seen between harmonic degree 150 and 250 mainly. The results also show how the increased availability of GOCE data improves the models.

To quantify the improvements in the modelling and the qualities of the GOCE models, accumulated differences between GOCE geoid models and DTU13MSS from harmonic degree 100 to 200 have been computed. This was done using 23 geoid models. As expected, the release 5 modes together with the combinations are producing the lowest values.

6. POSITIVE IMPACT OF GOCE FOR HIGH RESOLUTION MDT

The small scales (less than 100 km) missing in the MDT computing from satellite only geoid models can be brought either by the use of combined geoid model or by the use of oceanic in-situ data to compute high resolution MDT.

6.1. Combined geoid models (MDT DTU13)

As mentioned above the combination of satellite information with terrestrial information about the gravity filed may provide the mean for a computation of Earth gravity models having a much higher resolution. As an example the EGM2008 resolves the gravity field up to harmonic degree and order 2190 which roughly corresponds to a resolution of about 10 km. It is important to emphasize that this enhanced resolution in the marine areas are obtained using gravity data obtained from satellite altimetry. Though being a very good approximation to the geoid, the altimeter data is observations

of the sea surface height that has been converted into gravity anomalies. Hence, being converted back to geoid, those models will return information about the mean sea surface.

When computing the mean dynamic topography the experiences obtained using the GRACE models and the EGM2008 showed that the removal of shorter scale geoid signals not recovered by the satellite data substantially reduced those parts of the MSS-geoid differences that had to be filtered out. Also, the differences show a much more isotropic behaviour globally. Both the reduction of the short wavelengths and the smaller variation from region to region make the filtering a much easier process to complete successfully.

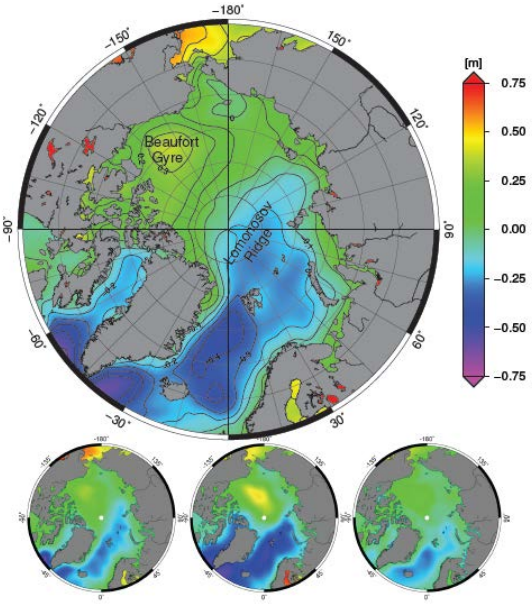

Figure 28: The DTU13MDT (height in meters) for the Arctic Ocean (upper figure). The lower figure shows the MDT computed from 3 years average of the GECCO, the MICOM, and University of Washington PIO (bottom left to right) hydrodynamic MDT

Figure 22 shows an example where the raw (unfiltered) MSS-geoid differences are shown when a satellite only model (in this case the DIR r5) and when a combined geoid model (in this case the EIGEN-6C3) are used. Clearly, by visual inspection, the differences obtained using the combined model are much smoother. As already discussed, in Figure 24 the respective power spectra are shown. Again, it is quite obvious that the combined geoid model removes most of the differences associated with wavelengths shorter than 0.6 cycles per degree (corresponding roughly to harmonic degree and order 220).

The DTU13MDT has been derived using the DTU13MSS and the EIGEN-6C3 geoid model [21]. The method is described in [22], [23] and [24]. The model is shown in Figure 28 for the Arctic Region.

6.2. Combined Mean Dynamic Topography (MDT CNES-CLS)

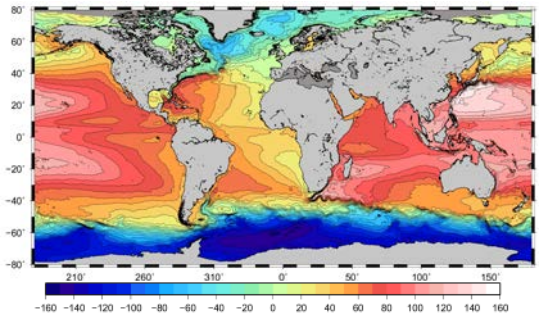

Figure 29: Mean Dynamic Topography CNES-CLS13 (cm)

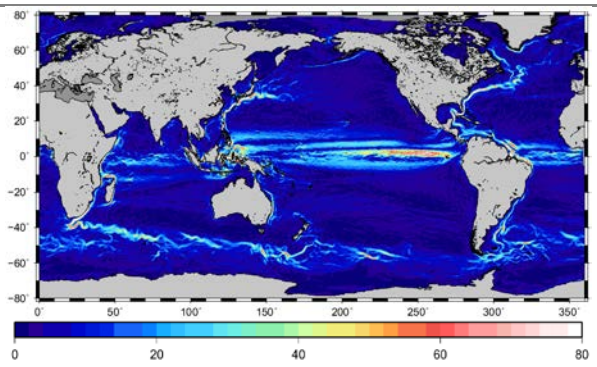

Figure 30: Intensity of the mean geostrophic current associated to the CNES-CLS13 MDT (cm/s)

Instead of using gravimetry data to add small scales to geoid model and then compute high resolution MDT; in-situ oceanic data can be combined with geodetic MDT computed from satellite only geoid model to compute high resolution combined MDT. For the computation of the CNES-CLS13 MDT, [19] compute first a geodetic MDT: they substract the geoid model DIR4 from CNES-CLS11 MSS and filter this difference with an optimal filter, this step end up with the so called "first guess". Beside, oceanic in-situ data are used to compute mean currents (from drifter currents as described in section 4.1) and mean dynamic topography from temperature and salinity profiles. Finally, geodetic MDT and in-situ data are combined thought multivariate objective analysis to end up with the CNES-CLS13 MDT (Figure 29) and associated mean current (Figure 30).

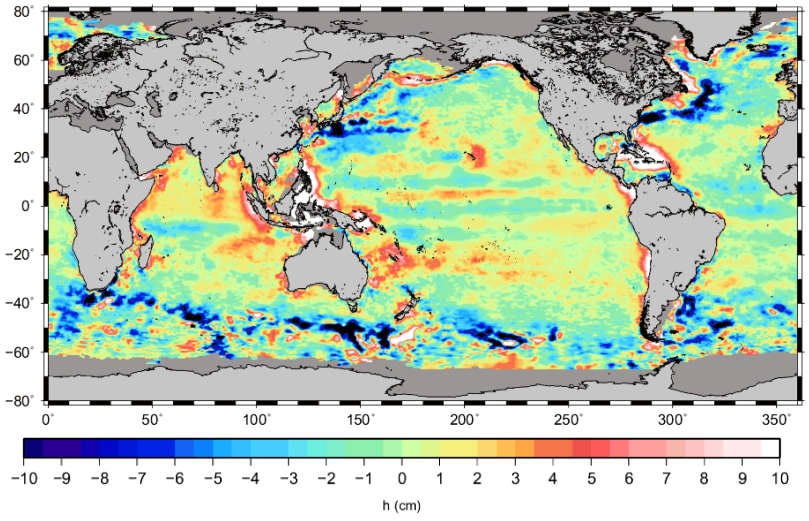

Figure 31: Difference between CNES_CLS13 and CNES_CLS09 MDTs

For the previous release of the CNES-CLS MDT (the CNES-CLS09), the first guess was computed from a GRACE geoid model, then part of the difference between the CNES-CLS09 and the CNES-CLS13 are due to improvement of GOCE over GRACE.

The absolute differences between CNES-CLS13 and CNES-CLS09 MDTs are around 13 cm in western boundary currents and circumpolar current (Figure 31) mainly due to improvement in the in-situ

processing for the CNES-CLS13. Moreover we can point out differences higher than 15 cm around the Bahamas and the Indonesia. This is mainly due to improvement of GOCE over GRACE.

In order to further investigate the impact of the newly computed CNES-CLS13 MDT (in thus GOCE), we have use it to compute the North Atlantic Meridional Overturning Circulation, and compared our result to the results obtained with the previous CNES-CLS09 MDT.

In the ocean, the warm tropical waters flow northward losing heat toward the atmosphere and becoming denser. At high latitudes, in the Atlantic, this water dives and goes back to lower latitudes flowing in the deep ocean. Thus, this Meridional Overturning Circulation (MOC) exchanges heat with the atmosphere, that is why it is very important for climate understanding.

At 26.5°N, the maximum strength of the Atlantic Meridional Overturning Circulation (AMOC) can be divided into three components:

1- the Florida western boundary transport that is monitored thanks to a telephonic cable (Larsen & al., 1992),

2- the meridional Ekman transport integrated from the Bahamas to Africa and computed from the zonal wind stress τ^x (from ERA INTERIM reanalysis - Simmons et al., 2007), the Coriolis parameter f and the water density following Equation 2:

$$T^y_{ekman} = -\frac{\tau^x}{f\rho}$$

Equation 2

3- the interior geostrophic transport computed by integrated 3D meridional geostrophic velocities from Bahamas to Africa and from the surface to 1 000 m.

The meridional geostrophic velocities at depth z_i $v_g(z_i)$ is computed following the method of Mulet et al. (2012b). Briefly it is based on the thermal wind equation (Equation 3):

$$v_g(z = z_i) = v_g(z = 0) - \frac{g}{f\rho}\int_0^{z_i} \frac{\partial \rho}{\partial x} dz$$

Equation 3

Where g is the gravity, f the Coriolis parameter, p the water density and v_g (z = 0) the geostrophic velocity at the sea surface. The density is given by temperature and salinity ARMOR3D field (Guinehut & al., 2012) and the velocity at the surface is deduced by geostrophy from altimetry (SLA + MDT). Thus, the MDT has an impact in the AMOC computation.

The mean interior geostrophic transport calculated over 2006 was -7 Sv when using the CNES-CLS09 MDT while it is -12 Sv with the CNES-CLS13 MDT. The RAPID-MOCHA array (Kanzow & al., 2007) gives an independent estimate of -14 Sv thanks to moorings that monitor temperature, salinity and currents. The new MDT is in good agreement with RAPID-MOCHA estimate and represents a significant improvement compared with the CNES-CLS09 MDT.

The interior geostrophic transport is negative (i.e. southward), this is expected when looking at Figure 32 because the MDT gradient is increasing westward (leading to a southward transport by geostrophy). However, the zonal gradient (difference between MDT east and west of the bassin) at 26.5°N is lower in the CNES-CLS09 than in the CNES-CLS13 because of a negative anomaly in CNES-CLS09 according with Figure 31, leading to a southward interior geostrophic transport lower by 5 Sv. As discussed above, this anomaly in the CNES-CLS09 MDT was due to the processing of the GRACE-based first guess. The use of the higher resolution GOCE based first guess is responsible for this significant improvement of the CNES-CLS13 MDT over the previous solution.

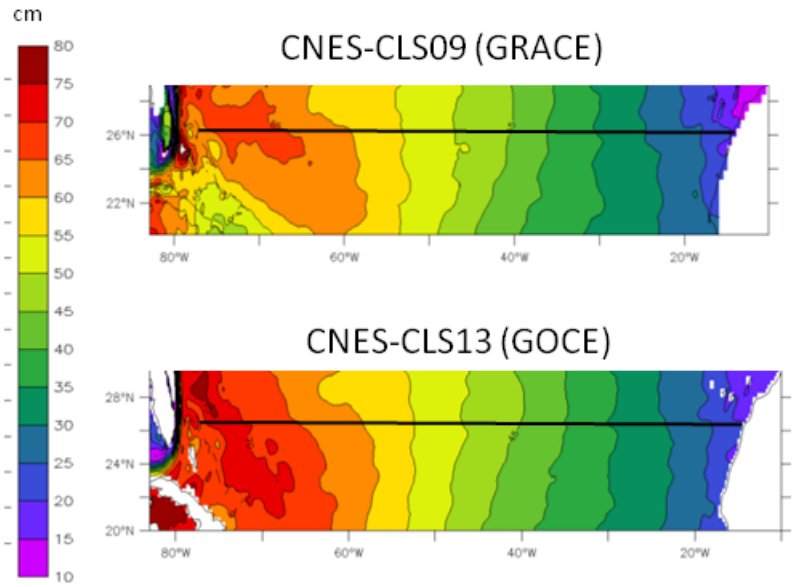

Figure 32: (top) CNES-CLS09 (bottom) CNES-CLS13 MDTs around the 26.5°N section in the Atlantic from Florida to Africa (cm)

7. CONCLUSION

This study shows the positive impact of using a GOCE based MDT for assimilation and how GOCE improves the computation of MDT compared with GRACE. The optimal resolution of GOCE MDT is between 100 and 125 km. Also we show how GOCE data help to improved combined geoid model between 100 and 200 km. GOCE is very useful to compute combined geoid model and combined MDT as DTU13 and CNES-CLS13 MDTs.

Thus GOCE is very useful for oceanographic application. First because it resolves smaller scales than previous gravimetric mission (i.e. GRACE). But also it resolves scales down to 100 km with a good accuracy helping to improve the products that already resolve such scale (combined geoid model, high resolution combined MDT and MDT from numerical model).

8. REFERENCES

[1] Schaeffer, P., Y. Faugère, J. F. Legeais, A. Ollivier, T. Guinle, N. Picot. The CNES_CLS11 Global Mean Sea Surface Computed from 16 Years of Satellite Altimeter Data, Marine Geodesy, Jason-2 special issue, 2012.

[2] Bruinsma, S., Förste, C., Abrykosov, O., Lemoine, J.-M., Marty, J.-C., Mulet, S., Rio, M.-H., Bonvalot, S. (2014): ESA's satellite-only gravity field model via the direct approach based on all

GOCE data. - Geophysical Research Letters, 41, 21, p. 7508-751.

[3] Andersen, O.B. (2010), The DTU10 Gravity field and Mean sea surface, Second international symposium of the gravity field of the Earth (IGFS2), Fairbanks, Alaska..

[4] Pail, R., H. Goiginger, W. Schuh, E. Höck, J.M. Brockmann, T. Fecher, T. Gruber, T. Mayer-Gürr, J. Kusche, A. Jäggi, and D. Rieser (2010), Combined satellite gravity field model GOCO01S derived from GOCE and GRACE, Geophys. Res. Lett., 37, L20314, doi:10.

[5] Bingham, R., K. Haines, and C.W. Hughes (2008), Calculating the Ocean's Mean Dynamic Topography from a Mean Sea Surface and a Geoid, Journal of Atmospheric and Oceanic Technology, 25, 1808-1823, doi:10.1175/2008JTECHO568.1.

[6] Marshall, J., C. Hill, L. Perelman, and A. Adcroft (1997), Hydrostatic, quasi-hydrostatic and nonhydrostatic ocean modelling, J. Geophys. Res., 102, 5733-5752.

[7] Köhl, A., and D. Stammer (2008), Decadal sea level changes in the 50-year GECCO-2 ocean synthesis, J. Clim., 21, 1876-1890.

[8] Siegismund, F., A. Köhl, and D. Stammer (2015), Impact of GOCE Gravity Data on the GECCO Ocean State Estimation, submitted to J. Geophys. Res.

[9] Stammer, D., C. Wunsch, R. Giering, C. Eckert, P. Heimbach, J. Marotzke, A. Adcroft, C. N. Hill, and J. Marshall (2002), The global ocean circulation during 1992-1997, estimated from ocean observations and a general circulation model, J. Geophys. Res.

[10] Lumpkin, R., and M.C. Pazos (2007), Measuring surface currents with Surface Velocity Program drifters: The instrument, its data, and some recent results, In: Lagrangian Analysis and Prediction of Coastal and Ocean Dynamics, Cambridge University Press.

[11] Niiler, P.P., N.A. Maximenko, and J.C. McWilliams (2003), Dynamically balanced absolute sea level of the global ocean derived from near-surface velocity observations, Geophysical Research Letters, 30(22), 2164, doi:10.1029/2003GL018628.

[12] Siegismund, F. (2013), Assessment of optimally filtered recent geodetic mean dynamic topographies, J. Geophys. Res. Ocean, 118, doi: 10.1029/2012JC008149.

[13] Grodsky, S.A., R. Lumpkin, and J.A. Carton (2011), Spurious trends in global surface drifter currents, Geophysical Research Letters, 38, L10606, doi:10.1029/2011GL047393.

[14] M.-H. R. e. S. B. Mulet S., “Accuracy of the preliminary GOCE GEOID models from an oceanographic perspective,” Marine Geodesy, 35:314–336, 2012 DOI: 10.1080/01490419.2012.718230, 2012.

[15] “Bruinsma S.L., Foerste C., Abrikosov O., Marty J.C., Rio M.-H., Mulet S., Bonvalot S. The new ESA satellite-only gravity field model via the direct approach,” Geophysical Research Letters, DOI: 10.1002/grl.50716, 2013.

[16] Kurtenbach, E., Mayer-Gürr T., and Eicker A. (2009), Deriving daily snapshots of the Earth's gravity field from GRACE L1B data using Kalman filtering, Geophys. Res. Lett., 36, L17102, doi:10.1029/2009GL039564.

[17] Hansen D.V., Poulain P.-M., (1996): Quality Control and Interpolations of WOCE-TOGA Drifter Data. J. Atmos. Oceanic Technol., 13, 900–909.

[18] Rio, M.-H. and Hernandez, F., (2003): High-frequency response of wind-driven currents measured by drifting buoys and altimetry over the world ocean. Journal of Geophysical Research, 108(C8): 3283-3301.

[19] Rio M.-H , S. Mulet and N. Picot, 2014. Beyond GOCE for the ocean circulation estimate: Synergetic use of altimetry, gravimetry and in-situ data provides new insight into geostrophic and Ekman currents. GRL.

[20] SSALTO/DUACS (2014), User Handbook: MSLA and MADT Near-Real Time and Delayed Products, C.L.S., Ramonville St. Agne, France.

[21] Emery W. J. et R. E. Thomson (2001). Data Analysis Methods in Physical Oceanography : Second and Revised Edition. Elsevier.

[22] Förste, C., Bruinsma, S., Shako, R., Marty, J-C, Flechtner, F., Abrikosov, O., Dahle, C., Lemoine, J.-M., Neumayer, K.H., Biancale, R., Barthelmes, F., König, R., Balmino, G. (2011) EIGEN-6 - A new combined global gravity field model including GOCE data.

[23] Knudsen, P., R. Bingham, O. Andersen, M.H. Rio, Enhanced Mean Dynamic Topography and Ocean Circulation Estimation using GOCE Preliminary Models, J. of Geodesy, 2011, DOI 10.1007/s00190/011/04858.

[24] Andersen, O., P. Knudsen and L. Stenseng. The DTU13 MSS (Mean Sea Surface) and MDT (Mean Dynamic Topography) from 20 years of satellite altimetry. Advances in Space Research - submitted. Proceedings of IFGS meeting, Shanghai July 2014.

[25] Knudsen, P. and O. Andersen (2013), The DTU12MDT Global mean dynamic topography and ocean circulation model, Proceeding of the Living Planet symposium, Edinburgh, 2013, ESA SP-772. ESA ESTEC. Nordweik.

Appendix A - **List of acronyms**

ACC	Antarctic Circumpolar Current
AMSR	Advanced Microwave Scanning Radiometer
DIR	The direct method to compute geoid model
EOF	Empirical Orthogonal Function
GECCO	German contribution to the Estimating the Circulation and Climate of the Ocean
GOCE	Gravity field and steady-state Ocean Circulation Explorer
GRACE	Gravity Recovery and Climate Experiment
HPF	High level Processing Facility
MDT	Mean Dynamic Topography
MSS	Mean Sea Surface
OGCM	Ocean General Circulation Models
TIM	The time wise method to compute geoid model